

# The Momentum Equilibrium Principle: Foot Contact Stabilization With Relative Angular Momentum/Velocity

Dragomir N. Nenchev

**Abstract**—The spatial momentum relation of an under-actuated articulated multibody system on a floating base is a dynamic equilibrium relation between its coupling and relative momenta. The relative momentum is the difference between the system momentum and the momentum of the composite-rigid-body (CRB) that is obtained when the joints are locked. This relation is referred to as the momentum equilibrium principle.

The focus in this work is on the angular momentum component of the momentum equilibrium principle. It is clarified that the relative angular momentum component can be represented in terms of the so-called relative angular velocity that is used as a control input in a balance controller. The balance controller proposed here is a whole-body controller that has independent inputs for center of mass (CoM) velocity and base-link angular velocity control. In addition, the relative angular velocity control input endows the controller with the unique property of generating an appropriate upper-limb motion that can stabilize the system momentum. More specifically, it is shown that when the relative angular velocity is derived from the reaction null-space (RNS) of the system, it becomes possible to stabilize the unstable states with a rolling foot/feet.

The formulation is simple and yet quite efficient — there is no need to modify the contact model to account for the transitions between the stable and unstable contact states. There is also no need to command the upper-limb motion directly. A few simulation examples are presented to demonstrate and discuss the properties of the controller.

## I. INTRODUCTION

The concept and realization of a balance controller based on the spatial momentum of a humanoid robot was introduced by Kajita et al. [1] fifteen years ago. The essence of the proposed *resolved momentum control* approach was to specify a reference *centroidal spatial momentum* and a reference motion trajectory for one of the end links, e.g. of the swing-leg foot, and resolve the spatial momentum equation for the joint velocity of the whole body via a local two-subtask constrained optimization approach, similar to that used in the kinematic redundancy resolution [2], [3]. The resolved momentum framework was the result of a pioneering effort toward a velocity-based *whole-body* balance control. The control law formulation was flawed, however, since the reference base-link twist was constrained by the null space of the main subtask. This led to an undesirable trunk rotation. In addition, task conflicts occurred that led to instabilities.

The important role of the *centroidal angular momentum* and its rate of change in balance control of humanoid robots was discussed in [4]. It was shown that the presence of

The author is with the Graduate School of Engineering, Tokyo City University, Tamazutsumi 1-28-1, Setagaya-ku, Tokyo 158-8557, Japan. nenchev@ieee.org

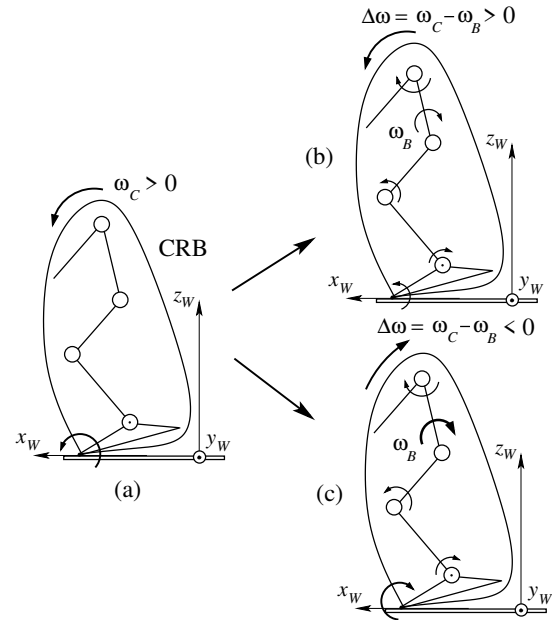


Fig. 1. Stabilization with the relative angular velocity (RAV)  $\Delta\omega$ . (a): An unstable state of the CRB (joints locked) with positive system angular velocity ( $\omega_C > 0$ ). (b): The system cannot be stabilized when the RAV is in the same direction as the system angular velocity. (c) A necessary condition for system stabilization is to generate a RAV in the direction opposite to the system angular velocity.

centroidal angular momentum is equivalent to shifting the application point of the ground reaction force (GRF) to a special point called the *centroidal moment pivot* (CMP) [5]. Further insight into the role of the angular momentum component and its relation to the widely used inverted pendulum models was provided in [6], [7] with a simple inverted pendulum plus a *reaction wheel* model. Since then, a number of balance controllers with angular momentum control components have been developed, e.g. [8]–[16], which is not an exhaustive list. The most recent results in balance control [15], [17], [18] have confirmed the importance of the centroidal angular momentum, not only for walking on a flat ground, but also while stepping on a highly irregular terrain. From this brief overview it can be concluded that centroidal angular momentum control is an indispensable component in the whole-body balance control of a humanoid robot.

In this work it is argued that although necessary, the centroidal angular momentum balance control approach is not sufficient. This hypothesis is based on the fact that the centroidal angular momentum can be expressed as the sum of two components: the composite rigid body (CRB)

component and the coupling angular momentum one [19]. The CRB component characterizes the behavior of the robot when all joints are locked. The links are then “frozen” in a particular configuration that determines the CoM and the inertia tensor of the CRB [20]. The coupling angular momentum component, on the other hand, depends on the joint rates; the joint rates are mapped via the coupling inertia matrix<sup>1</sup> to the centroidal angular momentum. The role of the coupling angular momentum component and the closely related concept of the *reaction null-space* (RNS) in the design of controllers for various underactuated robots on a floating-base, e.g. free-floating space robots, manipulators mounted on a flexible base and macro-mini manipulators (i.e. a small-size manipulator mounted at the tip of a large-size one) is discussed in [19].

The aim of this work is, first of all, to highlight the existence of the momentum equilibrium principle for floating-base robots. From this principle, the relative character of balance control can be deduced. The relative character of balance control with the (linear) momentum component has been exploited in the so-called zero moment point (ZMP) manipulation type controllers [23], [24] that make use of a well-known CoM/ZMP relation. This is also the case with the more recently introduced ICP/CMP [18] and DCM/VRP [17] type controllers<sup>2</sup>. On the other hand, the relative character of angular momentum-based balance control has not been discussed yet. It will be shown here that relativity in terms of angular momentum gives rise to two independent control inputs; one of them ensures the control of the net (the system) momentum, the other one controls the rotation of the floating base. As already noted, advanced balance control relies on an appropriate control of the system angular momentum to ensure walking on irregular terrain and to deal with foot rotations, as shown e.g. in [15], [18]. The system angular momentum control is achieved thereby with upper-body rotation. Note, however that then, the rotation of the trunk cannot be controlled in an independent way. In contrast, in the balance controller proposed in this work, the trunk rotation will be cast as a control task that is independent from the system angular momentum control task. The latter is achieved with an appropriate motion of the upper limbs. This leads to a significant advantage: the trunk can be used e.g. to accommodate an external disturbance without deteriorating thereby the system angular momentum control. In this way, the proposed balance controller is endowed with the unique property of complying with an external disturbance and, *in the same time*, of restoring the balance when the foot/feet have begun to roll.

Furthermore, it will be shown that the proposed balance controller can be represented in terms of angular velocity which leads to a simple structure. As a result, we obtain a controller that is also very efficient from the computational

<sup>1</sup>The coupling-inertia matrix is a coordinate form representation of the so-called *mechanical connection*. This map plays a substantial role in the modeling and control of underactuated systems in general [21], [22].

<sup>2</sup>ICP, DCM and VRP stand for “instantaneous capture point,” “divergent component of motion” and “virtual repellent point,” respectively.

point and that does not require a general solver.

Finally, it should be noted that although useful for position-controlled humanoid robots, a velocity-based balance controller has its inherent limits; it cannot account for the distribution of the body wrench, for example. A companion work [25] discusses the design of a balance controller that is based on the *rate of change* of the coupling angular momentum. This controller has the capability to deal with external disturbances of impulsive character and also, to distribute the body-wrench in a meaningful way.

This work is organized as follows. Section II gives the background and introduces the notations. In Section III, the momentum equilibrium principle is introduced. In Section IV, the CRB motion trajectory tracking task and its resolution are discussed. Section V introduces balance control with the relative angular velocity. In Section VI, the stabilization of the contacts at the feet is explained. Section VII presents a case study for balance control on a balance board. Finally, in Section VIII the conclusions are given.

## II. BACKGROUND AND NOTATION

### A. Generalized coordinates and quasivelocity

The generalized coordinate vector of a floating-base robot is denoted by  $\mathbf{q} = (\mathcal{X}_B, \boldsymbol{\theta})$ ;  $\boldsymbol{\theta} \in \mathfrak{R}^n$  stands for the joint variable vector,  $\mathcal{X}_B \in SE(3)$  is the position and orientation of the (non-actuated) base (or root) link. The generalized velocity is defined as a *quasivelocity*, i.e. as a velocity expressed relative to a configuration-dependent frame [26]. Note that the quasivelocity is not necessarily the time derivative of the generalized coordinates. Let  $\mathcal{V}_B = [\mathbf{v}_B^T \ \boldsymbol{\omega}_B^T]^T$  denote the twist of the base link;  $\mathbf{v}_B, \boldsymbol{\omega}_B \in \mathfrak{R}^3$  are the velocity of a fixed point on the base-link (e.g. the origin of the coordinate frame) and the angular velocity, respectively. These and all other quantities are expressed in the inertial frame. Furthermore, let  $\mathcal{V}_M = [\mathbf{v}_C^T \ \boldsymbol{\omega}_B^T]^T$  denote a twist of “mixed” character, where  $\mathbf{v}_C$  is the velocity of the CoM of the robot. Two quasivelocity vectors can then be specified as  $\dot{\mathbf{q}}_B = [\mathcal{V}_B^T \ \dot{\boldsymbol{\theta}}^T]^T$  and  $\dot{\mathbf{q}}_M = [\mathcal{V}_M^T \ \dot{\boldsymbol{\theta}}^T]^T$ . Note that there is some abuse in the notation: the over-dot in  $\dot{\mathbf{q}}_{(\circ)}$  does not necessarily imply the integrability of this quantity.

### B. The composite rigid body (CRB)

When the joints of the floating-base robot are locked at a given configuration  $\mathbf{q}$ , the robot behaves as a CRB. The centroidal spatial momentum of the CRB is defined as  $\mathcal{L}_C = [\mathbf{p}^T \ \mathbf{l}_C^T]^T$  where  $\mathbf{p} = M\mathbf{v}_C$  and  $\mathbf{l}_C = \mathbf{I}_C\boldsymbol{\omega}_B$  denote the linear and the centroidal angular momentum components, respectively,  $M$  is the total mass and  $\mathbf{I}_C(\mathbf{q}) \in \mathfrak{R}^{3 \times 3}$  stands for the centroidal inertia tensor of the CRB. With this notation, the spatial momentum of the CRB can be represented as

$$\mathcal{L}_C(\mathbf{q}, \mathcal{V}_M) = \mathbb{M}_C(\mathbf{q})\mathcal{V}_M \quad (1)$$

where

$$\mathbb{M}_C(\mathbf{q}) \equiv \begin{bmatrix} M\mathbf{E} & \mathbf{0} \\ \mathbf{0} & \mathbf{I}_C(\mathbf{q}) \end{bmatrix} \in \mathfrak{R}^{6 \times 6}$$

is the spatial inertia tensor of the CRB;  $\mathbf{E}$  denotes the identity matrix.

### C. The system and the coupling spatial momenta

The spatial momentum of the floating-base system can be expressed in different ways depending on the type of the quasivelocity. When expressed in terms of the mixed quasivelocity, for example, the *system spatial momentum* assumes the form:

$$\begin{aligned}\mathcal{L}_C(\mathbf{q}, \dot{\mathbf{q}}_M) &= \mathcal{L}_{CM}(\mathbf{q}, \mathcal{V}_M) + \mathcal{L}_{C\theta}(\mathbf{q}, \dot{\boldsymbol{\theta}}) \\ &= \mathbb{M}_C(\mathbf{q})\mathcal{V}_M + \mathbf{H}_{CM}(\mathbf{q})\dot{\boldsymbol{\theta}} \\ &= \begin{bmatrix} M\mathbf{E} & \mathbf{0} \\ \mathbf{0} & \mathbf{I}_C(\mathbf{q}) \end{bmatrix} \begin{bmatrix} \mathbf{v}_C \\ \boldsymbol{\omega}_B \end{bmatrix} + \begin{bmatrix} \mathbf{0} \\ \mathbf{H}_C(\mathbf{q}) \end{bmatrix} \dot{\boldsymbol{\theta}}.\end{aligned}\quad (2)$$

From the last term on the r.h.s. it is apparent that only the angular momentum component depends on the joint velocity;  $\mathcal{L}_{CM}(\mathbf{q}, \dot{\boldsymbol{\theta}}) = \mathbf{H}_{CM}(\mathbf{q})\dot{\boldsymbol{\theta}}$  and  $\mathbf{H}_C(\mathbf{q})\dot{\boldsymbol{\theta}}$  represent the *coupling spatial momentum* and the *coupling angular momentum* of the robot, respectively. Matrix  $\mathbf{H}_C(\mathbf{q})$  stands for the *coupling-inertia matrix* w.r.t. the angular motion — a coordinate form representation of the so-called *mechanical connection* [21], [22]. The system spatial momentum  $\mathcal{L}_C(\mathbf{q}, \dot{\mathbf{q}}_M)$  should be distinguished from the CRB spatial momentum  $\mathcal{L}_{CM}(\mathbf{q}, \mathcal{V}_M)$ ; they are not equal unless the joints are locked, or unless a special control is applied s.t.  $\dot{\boldsymbol{\theta}} \rightarrow \mathbf{0}$  throughout the motion.

Furthermore, from (2) it is apparent that the (linear) momentum component, besides being independent from the joint velocity, is also independent from the angular velocity of the base link. This property yields an advantage in balance controller design as clarified in [27], see also [28]. Note that in the analysis in [29], [30], as well as in the resolved momentum controller [1], the base quasivelocity  $\dot{\mathbf{q}}_B$  was employed. In this case, there is a coupling between the joint velocity and the (linear) momentum; this complicates the design of the balance controller. Indeed, the centroidal momentum controller in [15] suffered from the coupling problem, as did the resolved momentum controller. In both cases, a trade-off control policy had to be employed and thus, no rigorous stability proof could be devised. This problem can be avoided when the centroidal spatial momentum is expressed in terms of the mixed quasivelocity, as above.

### D. System angular velocity, centroidal twist and centroidal quasivelocity

The coupling-inertia matrix  $\mathbf{H}_C$  in (2) can be represented as the product of the CRB inertia tensor and a Jacobian-like quantity. Indeed, noting that the CRB inertia tensor is positive-definite, we can premultiply the lower part of (2) with  $\mathbf{I}_C^{-1}$  to obtain:

$$\mathbf{I}_C^{-1}\mathbf{l}_C = \boldsymbol{\omega}_B + \mathbf{I}_C^{-1}\mathbf{H}_C\dot{\boldsymbol{\theta}}.\quad (3)$$

Now we can define the quantities  $\boldsymbol{\omega}_C \equiv \mathbf{I}_C^{-1}\mathbf{l}_C$  and  $\mathbf{J}_\omega(\boldsymbol{\theta}) \equiv \mathbf{I}_C^{-1}\mathbf{H}_C$ . With this notation, the last equation can be rewritten as

$$\boldsymbol{\omega}_C = \boldsymbol{\omega}_B + \mathbf{J}_\omega(\boldsymbol{\theta})\dot{\boldsymbol{\theta}}.\quad (4)$$

This relation represents the instantaneous angular motion of the floating-base robot. Note that although  $\boldsymbol{\omega}_C$  has the meaning of an angular velocity, it does not associate with a specific physical body;  $\boldsymbol{\omega}_C$  will be therefore referred to as the *system angular velocity*. We can also define the *centroidal twist* and the *centroidal quasivelocity* as  $\mathcal{V}_C = [\mathbf{v}_C^T \ \boldsymbol{\omega}_C^T]^T$  and  $\dot{\mathbf{q}}_C = [\mathcal{V}_C^T \ \dot{\boldsymbol{\theta}}^T]^T$ , respectively.

For the sake of completeness, it should be noted that when the centroidal quasivelocity notation is employed, both the linear and the angular components of the spatial momentum become independent from the joint velocity. In other words, with the centroidal quasivelocity, only the CRB spatial momentum can be exposed, i.e.

$$\mathcal{L}_C(\mathbf{q}, \dot{\mathbf{q}}_C) = \mathcal{L}_C(\mathbf{q}, \mathcal{V}_C) = \mathcal{L}_C(\mathbf{q}, \mathcal{V}_M).\quad (5)$$

### E. Instantaneous motion constraints

The instantaneous motion of the humanoid robot is constrained by  $c$  constraints at the contact joints, such that

$$\mathbb{C}_c^T(\mathbf{q})\mathcal{V}_M + \mathcal{J}_c(\mathbf{q})\dot{\boldsymbol{\theta}} = \mathbf{0}.\quad (6)$$

$\mathbb{C}_c(\mathbf{q}) \in \mathbb{R}^{6 \times c}$  and  $\mathcal{J}_c(\mathbf{q}) \in \mathbb{R}^{c \times n}$  denote the contact map and the Jacobian in the constrained-motion directions, respectively. Furthermore, there are  $\eta$  unconstrained-motion directions. The respective instantaneous motion is determined by:

$$\mathbb{C}_m^T(\mathbf{q})\mathcal{V}_M + \mathcal{J}_m(\mathbf{q})\dot{\boldsymbol{\theta}} = \bar{\mathbf{v}}^m.\quad (7)$$

$\mathbb{C}_m(\mathbf{q}) \in \mathbb{R}^{6 \times \eta}$  and  $\mathcal{J}_m(\mathbf{q}) \in \mathbb{R}^{\eta \times n}$  denote the contact map and the Jacobian in the mobility (unconstrained-motion) directions, respectively.  $\bar{\mathbf{v}}^m \in \mathbb{R}^\eta$  are desired twist components for the instantaneous end-link motion along the unconstrained motion directions. Considering the hands and feet,  $c + \eta = 24$ . The general case  $n > c + \eta$ , is assumed here which means that the robot may comprise kinematically redundant limbs. A detailed derivation of the above relations is presented in [31].

## III. THE MOMENTUM EQUILIBRIUM PRINCIPLE IN FLOATING-BASE ROBOTICS

Using (1) and (5), the system spatial momentum (2) can be rewritten as:

$$\mathbf{H}_{CM}\dot{\boldsymbol{\theta}} = \mathbb{M}_C\mathcal{V}_C - \mathbb{M}_C\mathcal{V}_M.\quad (8)$$

This relation clearly shows that with the joint velocity, a finite difference in momentum can be controlled: the *system spatial momentum*,  $\mathbb{M}_C\mathcal{V}_C$ , minus the CRB spatial momentum,  $\mathbb{M}_C\mathcal{V}_M$ . The difference will be henceforth referred to as the *relative momentum* of the floating-base system.

The above equation represents the momentum equilibrium principle in balance control of a humanoid robot: *the coupling momentum is always in a dynamic equilibrium with the relative momentum*. This principle is quite helpful in balance controller design. In fact, it has been exploited throughout the years, but only with regard to the linear momentum component, first with the so-called ZMP manipulation type controllers [23], [24] and more recently, with the ICP/CMP

[18] and the DCM/VRP [17] type controllers. In what follows, it will be shown how to employ this principle also with regard to the angular momentum component.

Before doing so, we will recast the momentum equilibrium principle in terms of spatial velocity. This can be done in a straightforward manner since the CRB spatial inertia tensor is positive definite. Premultiply (8) by  $\mathbb{M}_C^{-1}$  to obtain

$$\mathbb{M}_C^{-1} \mathbf{H}_{CM} \dot{\boldsymbol{\theta}} = \mathcal{V}_C - \mathcal{V}_M \equiv \Delta \mathcal{V}. \quad (9)$$

The term on the left hand-side, referred to as the *coupling spatial velocity*, is in balance with the *relative spatial velocity*  $\Delta \mathcal{V}$  on the right hand-side. When represented component-wise, the above equilibrium relation assumes the form

$$\mathbf{0} = \mathbf{v}_{C_R} - \mathbf{v}_{C_I}, \quad (10)$$

$$\mathbf{J}_\omega \dot{\boldsymbol{\theta}} = \boldsymbol{\omega}_C - \boldsymbol{\omega}_B \equiv \Delta \boldsymbol{\omega}. \quad (11)$$

From the upper equation it is apparent that the coupling CoM velocity is zero. It is also apparent that the CoM velocity can be interpreted in two ways:  $\mathbf{v}_{C_I}$  is of *inertial* origin, while  $\mathbf{v}_{C_R}$  stems from the *net* system twist that is of *reactive* origin. The origins can be distinguished only when the CoM motion is expressed in terms of acceleration, though [25]. The velocities are indistinguishable, thus:  $\mathbf{v}_{C_I} = \mathbf{v}_{C_R} = \mathbf{v}_C$ ,  $\Delta \mathbf{v}_C = \mathbf{0}$ . Next, note that the lower equation expresses a dynamic equilibrium in the angular velocities: the *coupling angular velocity*  $\mathbf{J}_\omega \dot{\boldsymbol{\theta}}$  is in balance with the *relative angular velocity* (RAV)  $\Delta \boldsymbol{\omega} \neq \mathbf{0}$ . One arrives then at the important conclusion that *the angular velocity of the system and that of the base link can be specified in an independent way*.

The RAV plays an important role in the stabilization of unstable states. The concept is outlined in Fig. 1, the details will be given in Section VI.

#### IV. CRB MOTION TRAJECTORY TRACKING TASK

Since the angular velocity of the base link can be specified in an independent way, it becomes possible to assign a trajectory tracking task not only for the CoM trajectory, as in the existing balance controllers, but also for the angular trajectories of the base link. Note that the most advanced balance controllers that make use of the centroidal spatial momentum and its rate of change e.g. [15], [17], [18], did not provide means for tracking arbitrarily assigned angular trajectories of the base link (i.e. of the trunk); the motion of the trunk is determined solely by the outcome of the centroidal spatial momentum control subtask.

Given the reference trajectories of the CRB specified by  $\mathcal{V}_M^{ref}(t) = [(\mathbf{v}_C^{ref}(t))^T \ (\boldsymbol{\omega}_B^{ref}(t))^T]^T$ , an infinite set of constraint-consistent joint velocity solutions can be obtained from (6) as

$$\dot{\boldsymbol{\theta}}_1 = -\mathcal{J}_c^+ \mathbb{C}_c^T \mathcal{V}_M^{ref} + \mathbf{N}(\mathcal{J}_c) \dot{\boldsymbol{\theta}}_u. \quad (12)$$

The notation  $(\circ)^+$  stands for the pseudoinverse. The second term on the right-hand side is a null-space term:  $\mathbf{N}(\circ)$  denotes a projector onto the null space, in this case of the contact Jacobian. Joint velocity  $\dot{\boldsymbol{\theta}}_u$  is an arbitrary joint velocity that parameterizes the null space. The CRB reference

trajectories can be obtained from a conventional kinematic control law, e.g.

$$\mathbf{v}_C^{ref} = \mathbf{v}_C^{des} + K_{pC} \mathbf{e}_{pC}, \quad (13)$$

$$\boldsymbol{\omega}_B^{ref} = \boldsymbol{\omega}_B^{des} + K_{oB} \mathbf{e}_{oB}. \quad (14)$$

The notation  $(\circ)^{des}$  stands for a desired value,  $\mathbf{e}_{pC} = \mathbf{r}_C^{des} - \mathbf{r}_C$  and  $\mathbf{e}_{oB}$  denote the CoM position error and the base-link angular error, respectively. When the contacts at the feet are stable and the joint-space constraint Jacobian  $\mathcal{J}_c$  is full (row) rank, the control law (12) guarantees that  $\mathcal{V}_M(t) = \mathcal{V}_M^{ref}(t)$  asymptotically, in the same way as in the case of a fixed-base robot. Note that for the purpose of humanoid robot balance control, it would be preferable to replace  $\mathbf{v}_C^{ref}$  in (13) with a feedback control law that is based on the ICP/CMP relation.

The control input  $\dot{\boldsymbol{\theta}}_1$  is useful when the robot is in a double stance. When in a single stance, the tracking of the desired foot trajectories of the swing leg could be embedded as a lower-priority task. To this end, determine the arbitrary joint velocity vector  $\dot{\boldsymbol{\theta}}_u$  in (12) with the help of the instantaneous-motion equation (7). The control joint velocity assumes then the form:

$$\dot{\boldsymbol{\theta}}_2 = -\mathcal{J}_c^+ \mathbb{C}_c^T \mathcal{V}_M^{ref} + \bar{\mathcal{J}}_m^+ (\tilde{\mathcal{V}}^m)^{ref} + \mathbf{N}(\mathcal{J}_c) \mathbf{N}(\bar{\mathcal{J}}_m) \dot{\boldsymbol{\theta}}_u \quad (15)$$

where  $\bar{\mathcal{J}}_m = \mathcal{J}_m \mathbf{N}(\mathcal{J}_c)$  is the restricted end-link mobility Jacobian and

$$(\tilde{\mathcal{V}}^m)^{ref} = (\bar{\mathcal{V}}^m)^{ref} + \left( \mathcal{J}_m \mathcal{J}_c^+ \mathbb{C}_c^T - \mathbb{C}_m^T \right) \mathcal{V}_M^{ref}.$$

Reference  $(\bar{\mathcal{V}}^m)^{ref}$  comprises a nonzero component for the swing leg:

$$\mathcal{V}_{F_{SW}}^{ref} = \mathcal{V}_{F_{SW}}^{des} + \mathbf{K}_{F_{SW}} \mathcal{E}_{F_{SW}}, \quad (16)$$

the rest of its components are zeros. Subscript  $(\circ)_{F_{SW}}$  stands for the foot of the swing leg,  $\mathcal{E}_{F_{SW}}$  is the error twist,  $\mathbf{K}_{F_{SW}}$  is a p.d. feedback gain.

#### V. RELATIVE ANGULAR MOMENTUM/VELOCITY BALANCE CONTROL COMPONENT

The above controller cannot be directly employed when the contacts are destabilized. This problem can be alleviated by adding a control component for the system angular momentum. The additional control component can be designed with the RAV which is a function of the system angular velocity  $\boldsymbol{\omega}_C$ . To this end, insert (15) into (11) and solve for the arbitrary  $\dot{\boldsymbol{\theta}}_u$ . Then, insert back into (12) to finally obtain the enhanced control law as

$$\begin{aligned} \dot{\boldsymbol{\theta}} &= -\mathcal{J}_c^+ \mathbb{C}_c^T \mathcal{V}_M^{ref} + \bar{\mathcal{J}}_m^+ (\tilde{\mathcal{V}}^m)^{ref} + \bar{\mathcal{J}}_\omega^+ (\Delta \boldsymbol{\omega}^{ref} - \tilde{\boldsymbol{\omega}}) \\ &\quad + \mathbf{N}(\mathcal{J}_c) \mathbf{N}(\bar{\mathcal{J}}_m) \mathbf{N}(\bar{\mathcal{J}}_\omega) \dot{\boldsymbol{\theta}}_u^{ref} \\ &= \dot{\boldsymbol{\theta}}^c + \dot{\boldsymbol{\theta}}^m + \dot{\boldsymbol{\theta}}^{am} + \dot{\boldsymbol{\theta}}^n, \end{aligned} \quad (17)$$

where  $\Delta \boldsymbol{\omega}^{ref} = \boldsymbol{\omega}_C^{ref} - \boldsymbol{\omega}_B^{ref}$  and

$$\begin{aligned} \bar{\mathcal{J}}_\omega &= \mathbf{J}_\omega \mathbf{N}(\mathcal{J}_c) \mathbf{N}(\bar{\mathcal{J}}_m), \\ \tilde{\boldsymbol{\omega}} &= \mathbf{J}_\omega \left( -\mathcal{J}_c^+ \mathbb{C}_c^T \mathcal{V}_M^{ref} + \bar{\mathcal{J}}_m^+ (\tilde{\mathcal{V}}^m)^{ref} \right). \end{aligned}$$

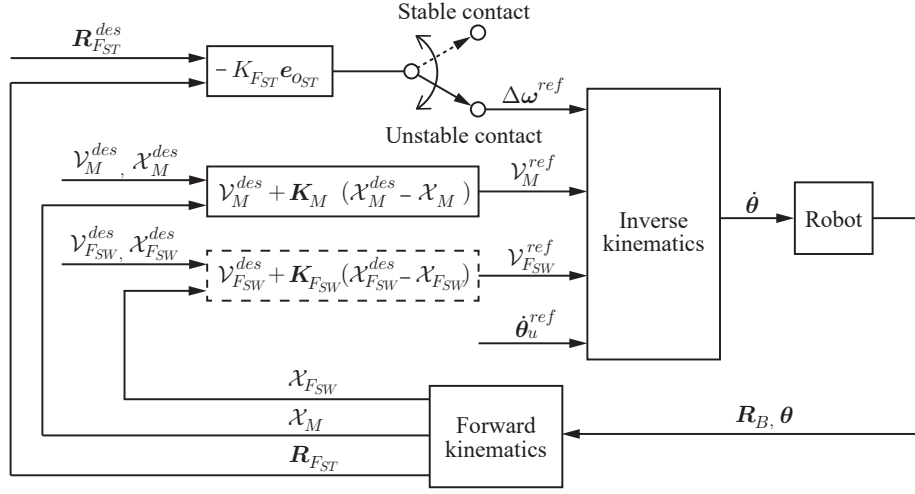


Fig. 2. Block diagram of an RAM/V controller that can be used to stabilize the feet contacts by an appropriate RAV input  $\Delta\omega^{ref}$ . The Inverse kinematics block calculates the control joint velocity in accordance with (17). The  $(\circ)_{FSW}$  components are used only when in a single stance. The  $\mathcal{X}(\circ)$  quantities collect positions and orientations in 3D, the latter being parametrized in any convenient form.

Reference  $\omega_B^{ref}$  is given in (14),  $\omega_C^{ref}$  will be specified in what follows. The control input  $\dot{\theta}$  is composed of four components arranged in a hierarchical order. The highest-priority component,  $\dot{\theta}^c$ , is used to control the instantaneous motion of the CRB, via the contact constraints. The desired CRB translational (i.e. of the CoM) and rotational (of the base link) motion is achieved via the movements in the leg(s). The rest of the control components are derived from within the null space  $\mathcal{N}(\mathcal{J}_c)$ . These components will not disturb the main (the CRB) control task. The role of the second component,  $\dot{\theta}^m$ , is to control the desired motion of the swing leg, when the robot is in a single stance. The role of the third component,  $\dot{\theta}^{am}$ , is to control the RAV (or equivalently the system angular velocity since  $\omega_B^{ref}$  has been specified) in a way to ensure an appropriate inertial coupling w.r.t. the desired CRB rotational motion. Note that such coupling can only be achieved via motion in the arms since the legs and the upper body are controlled by the first two components. The last, fourth component,  $\dot{\theta}^n$ , is used to enforce the joint velocity/angular constraints. To this end, the additional control input  $\dot{\theta}_u^{ref}$  can be determined e.g. by the gradient projection approach with the joint-limit avoidance potential function introduced e.g. in [32].

Note that when the robot is in a single stance and there is no desired motion task for the swing leg, the second component,  $\dot{\theta}^m$ , becomes irrelevant. The motion of the swing leg will then be determined by the angular momentum component  $\dot{\theta}^{am}$ . This means that the motion of the swing leg will contribute to the postural stabilization via the system angular momentum, as does the motion in the arms. This contribution plays an important role, e.g. when a large external disturbance is applied to the robot, since the leg has a significantly larger inertia than that of the arms [25].

The above controller will be referred to as the *relative angular momentum/velocity (RAM/V) controller*. The block diagram is shown in Fig. 2. The desired values for the CoM

motion, the base-link rotation, the swing-leg motion and the system angular momentum can be specified in an *independent* way. The controller does not account for other important constraints, such as keeping the ZMP within the support polygon or the friction cone constraints. Nevertheless, using the RAV control input  $\Delta\omega^{ref}$ , the controller can stabilize the feet contacts after their destabilization, stemming e.g. from an external force or from self-destabilization when some of the desired inputs are specified in an improper way (e.g. a large CoM acceleration). Note that to avoid an overconstrained system, it is recommendable to use the RAV control input only when the contacts are unstable (this is shown with the switch in the block-scheme of the controller).

## VI. RNS-BASED STABILIZATION OF UNSTABLE FOOT CONTACTS

Assume the robot has been destabilized, either proactively or by an external force. This means that the foot (when in a single stance) or the feet (when in a double stance) have begun to roll. A swift action is required for contact stabilization. Such an action can be generated in a straightforward way with the RAM/V controller introduced in the last subsection. This will be explained with the help of the simple sagittal-plane model shown in Fig. 1. Assume the foot rolls around the toe tip counterclockwise s.t. the system angular speed  $\omega_C > 0$ . When the joints are locked, the angular speed of the system equals that of the CRB and of all other links:  $\omega_C = \omega_B = \omega_i, i \in \{1, n\}$ . As a consequence, the relative angular speed is zero:  $\Delta\omega = \omega_C - \omega_B = 0$ . When the robot links are allowed to rotate, in general the system angular speed will be different from that of the base link, and thus, the relative angular speed will be nonzero. For this particular example, when  $\Delta\omega > 0$ , the foot roll will persist and result in a fall. On the other hand, when  $\Delta\omega < 0$ , the foot will start rotating in the opposite (clockwise) direction resulting

in the recovery of the line contact, and eventually, of a stable posture.

Furthermore, note that by simply forcing the robot to behave as a CRB, a *neutral response* to a destabilization can be created. In other words, the respective joint motion will neither increase nor decrease the energy of the system. Such a response can be obtained by setting the reference system angular velocity as

$$\omega_C^{ref} = \omega_B^{ref} \Rightarrow \Delta\omega^{ref} = \mathbf{0}. \quad (18)$$

This means that the coupling angular momentum will be conserved at zero, with the following joint velocity:

$$\{\dot{\theta}_{RNS} \in \mathcal{N}(\mathbf{J}_\omega) : \dot{\theta} = \mathbf{N}(\mathbf{J}_\omega(\theta))\dot{\theta}_a, \forall \theta_a\}.$$

The null-space  $\mathcal{N}(\mathbf{J}_\omega(\theta))$  is referred to as the (angular momentum) *reaction null-space* (RNS) [19]. It is interesting to note that forcing the robot to behave as a CRB yields an arm rotation that is always in antiphase to the foot/CRB roll. As a consequence of the neutral response commanded via  $\dot{\theta}_{RNS}$ , a rocking-feet motion will be obtained. Note that the robot is completely “unaware” of this motion. Note also that there is no need to change the contact joint type (i.e. from line contact to point contact) in the instantaneous motion constraint (6).

Depending on the energy generated/absorbed during the destabilization, the rocking motion may diverge and result in a fall. In order to avoid this and to ensure the stabilization of the feet contacts, the energy has to be dissipated. This can be done with the help of the following feedback-type control law:

$$\Delta\omega^{ref} = -K_{o_F} e_{o_F}. \quad (19)$$

Here  $e_{o_F}$  is the foot orientation error and  $K_{o_F}$  is a p.d. feedback gain. The foot rotation angle is obtained from the base orientation measured by an IMU sensor and the leg joint angles measured by the joint encoders.

The above relations are demonstrated with simulations<sup>3</sup>. The *whole-body* model of a small-size humanoid robot HOAP-2 [34] was employed (we did not use the pitch joint in the trunk of the robot, though). The robot was placed on a flat ground in a symmetric posture, the feet being aligned. The initial posture was stabilized with the asymptotic CRB trajectory tracking control laws (13) and (14). Throughout the motion, the CoM was regulated at the initial position, using the feedback gain  $K_{p_C} = 100$ . The robot first destabilized itself by a fast forward bend in the hips. The forward bend was commanded with a desired hip-pitch angle of 0.2 rad that had to be achieved within the time interval  $0 \leq t \leq t_d$ , where  $t_d = 0.1$  s (we used a fifth-order spline). The feedback gain for base orientation during the destabilization was set at zero:  $K_{o_B}(t) = 0$ , ( $0 \leq t \leq t_d$ ).

First, the neutral response was simulated. To this end, after  $t = t_d$ , the base-link orientation feedback gain was gradually increased to enable the tracking of the desired orientation (the initial zero hip-pitch angle):  $K_{o_B}(t) = 100$ , ( $t_d \leq t \leq t_f$ ),

<sup>3</sup>The Choreonoid dynamic simulator [33] was used.

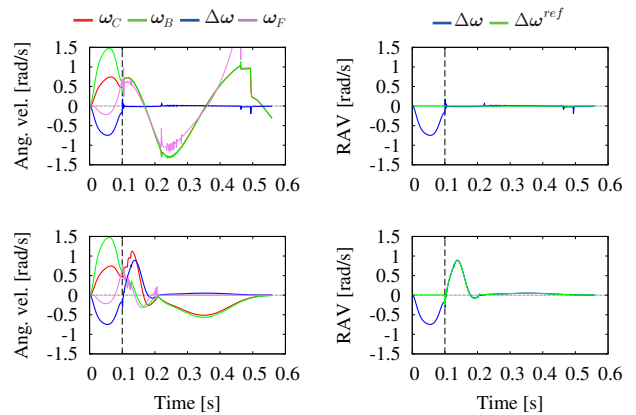


Fig. 3. Pitch angular speed data. The graphs in the top/bottom rows are for the response without/with feedback control. The end of the destabilization time interval is shown with the vertical dashed line.

where  $t_f = 1.0$  s. The data graphs for the pitch angular speeds are shown in the top row of Fig. 3. The end of the destabilization is shown with the vertical dashed line. During the destabilization,  $\omega_B > \omega_C$  and thus,  $\Delta\omega < 0$ . The angular speed of foot roll,  $\omega_F$ , was first negative then became positive (the rocking motion). After the destabilization, the RAV  $\Delta\omega \approx 0$  in accordance with the reference value. This determined the neutral response as a CRB. The rocking motion continued and resulted in a fall. The animated motion is shown in Part 1 of the accompanying video.

In the next simulation, after the destabilization, the reference RAV was determined from (19), with a constant feedback gain  $K_{o_F} = 100$ . From the graphs in the bottom line of Fig. 3 it is apparent that the rocking motion was quickly suppressed (at about  $t = 0.2$  s). Thereafter, the system angular speed followed that of the base. The robot arrived finally at the desired base orientation. The animated motion is shown in Part 2 of the accompanying video.

## VII. CASE STUDY: POSTURE STABILIZATION ON A BALANCE BOARD

The robot<sup>4</sup> was placed on a slightly damped (the damping constant was unity) balance board. High-friction contacts were employed to avoid a slip at the feet. The RAM/V controller with the RNS constraint was used to stabilize the unstable states attained whenever the CoM of the robot was displaced from the (unstable) set of equilibrium points, i.e. from the vertical passing through the center of rotation of the balance board. The CoM motion control task was regulation in the horizontal direction toward the equilibrium line. The base-link rotation task was also a regulatory one: keep the trunk upright. The stabilization of the posture was achieved with the reference RAV given in (18). The feedback gains were set at  $K_{p_C} = 100$  and  $K_{o_B} = 1$ .

Snapshots from the simulation are displayed in Fig. 4, the animated motion shown in Part 3 of the accompanying video. The graphs are shown in Fig. 5. Note that the initial

<sup>4</sup>The same robot model and simulation environment as in the previous simulation was used.

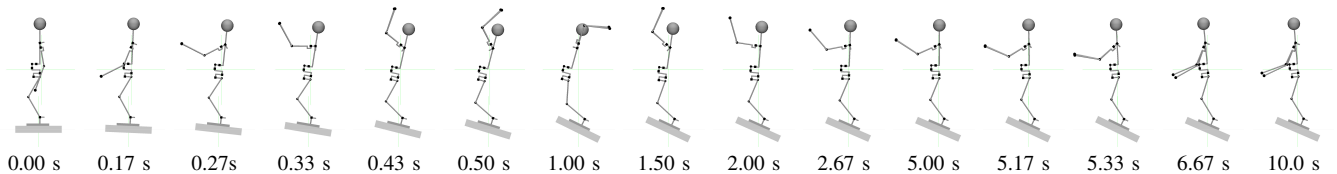


Fig. 4. Posture stabilization on a balance board under RAM/V plus RNS control. The initial posture is unstable since the CoM is displaced from the vertical passing through the center of rotation of the balance board. The posture is stabilized swiftly via the upper-limb motion (the trunk is commanded to keep its upright orientation). At  $t = 5$  s the robot self-destabilizes by a fast forward bend. The final posture at  $t = 10$  s represents a stable, static state.

posture was unstable. It took about five seconds to stabilize the posture. Immediately after the stabilization, the robot destabilized itself with a swift forward bent in the hips. Apparently, the RAM/V plus RNS controller could handle such type of destabilization as well, s.t. the robot arrived finally at a stable static posture.

Note that in this simulation, there was no need to employ the feedback control (19). The RNS input  $\Delta\omega^{ref} = \mathbf{0}$  was used throughout the motion. We found that this is related to the low feedback gain used for the trunk rotation. Further studies are needed in this direction.

### VIII. SUMMARY AND CONCLUSIONS

The theoretical contribution of this work is the formulation of the momentum equilibrium principle for floating-base robots. From this principle, the relative character of momentum balance was deduced. It was shown that the relativity relation is instrumental in finding an answer to the crucial question in balance control: “how to determine an appropriate centroidal angular momentum?”

It was shown how to harness the relativity of angular momentum in the form of the relative angular velocity (RAV) and to design a balance controller. The proposed RAM/V controller comprises the following unique properties: (1) enables the assignment of trunk motion in a desirable way, independently from the outcome of the CoM-based balance control task; (2) generates a meaningful arm motion; (3) stabilizes rolling foot/feet contacts. With a RAV that enforces a *reactionless motion*, i.e. a motion derived from the RNS, the controller is endowed with the capability to absorb relatively large disturbances. The formulation is simple and yet quite efficient; there is no need to modify the contact model to account for the transitions between the stable and unstable states. The controller is also very fast; there is no need to employ an iterative solver.

The performance of the RAM/V controller can be further improved by reformulating it in terms of acceleration, as the *relative angular acceleration* (RAA) controller presented in the companion paper [25]. It becomes then possible to inject *angular momentum damping* into the system. The damping ensures the convergence to a stable contact state, without the direct involvement of the foot rotation error as in the rolling foot example in the present paper. It also ensures a superior balance s.t. the robot is enabled to absorb high-energy impacts. We have already confirmed this for impacts that occur when a large external disturbance is applied to the upper body [25], when landing after jumping and when the

foot steps with high speed over an unknown obstacle. We believe that the method has a significant potential to be used in a number of other tasks, which we intend to explore in our future research.

### ACKNOWLEDGMENT

The simulation results, the videos and some of the figures were provided by Ryotaro Hinata and Takuma Nakamura.

### REFERENCES

- [1] Shuuji Kajita, Fumio Kanehiro, Kenji Kaneko, Kiyoshi Fujiwara, Kensuke Harada, Kazuhito Yokoi, and Hirohisa Hirukawa. Resolved momentum control: humanoid motion planning based on the linear and angular momentum. In *IEEE/RSJ International Conference on Intelligent Robots and Systems*, pages 1644–1650, Las, Vegas, Nevada, 2003.
- [2] Hideo Hanafusa, Tsuneo Yoshikawa, and Yoshihiko Nakamura. Analysis and control of articulated robot arms with redundancy. In *Prep. of the IFAC '81 World Congress*, pages 78–83, 1981.
- [3] M. S. Konstantinov, M. D. Markov, and D. N. Nenchev. Kinematic control of redundant manipulators. In *11th International Symposium on Industrial Robots*, pages 561–568, Tokyo, Japan, 1981.
- [4] Ambarish Goswami and Vinutha Kalleem. Rate of change of angular momentum and balance maintenance of biped robots. In *IEEE International Conference on Robotics and Automation*, pages 3785–3790, New Orleans, LA, USA, 2004.
- [5] M. B. Popovic, Ambarish Goswami, and Hugh Herr. Ground reference points in legged locomotion: Definitions, biological trajectories and control implications. *The International Journal of Robotics Research*, 24(12):1013–1032, dec 2005.
- [6] Jerry E Pratt. *Exploiting inherent robustness and natural dynamics in the control of bipedal walking robots*. PhD thesis, MIT, 2000.
- [7] Jerry Pratt, John Carff, S. Drakunov, and Ambarish Goswami. Capture point: A step toward humanoid push recovery. In *IEEE-RAS International Conference on Humanoid Robots*, pages 200–207, Genoa, Italy, dec 2006.
- [8] Muhammad Abdallah and Ambarish Goswami. A biomechanically motivated two-phase strategy for biped upright balance control. In *IEEE Int. Conf. on Robotics and Automation*, pages 1996–2001, Barcelona, Spain, 2005.
- [9] Taku Komura, Howard Leung, James Kuffner, Shunsuke Kudoh, and James Kuffner. A feedback controller for biped humanoids that can counteract large perturbations during gait. *IEEE International Conference on Robotics and Automation*, (April):1989–1995, 2005.
- [10] Hirohisa Hirukawa, Shizuko Hattori, Kensuke Harada, Shuuji Kajita, Kenji Kaneko, Fumio Kanehiro, Kiyoshi Fujiwara, and Mitsuharu Morisawa. A universal stability criterion of the foot contact of legged robots - adios ZMP. In *IEEE International Conference on Robotics and Automation*, number May, pages 1976–1983, 2006.
- [11] Shunsuke Kudoh, Taku Komura, and Katsushi Ikeuchi. Stepping motion for a human-like character to maintain balance against large perturbations. In *IEEE International Conference on Robotics and Automation*, pages 2661–2666, 2006.
- [12] Adriano Macchietto, Victor Zordan, and Christian R. Shelton. Momentum control for balance. *ACM Transactions on Graphics*, 28(3):80:1–80:8, 2009.

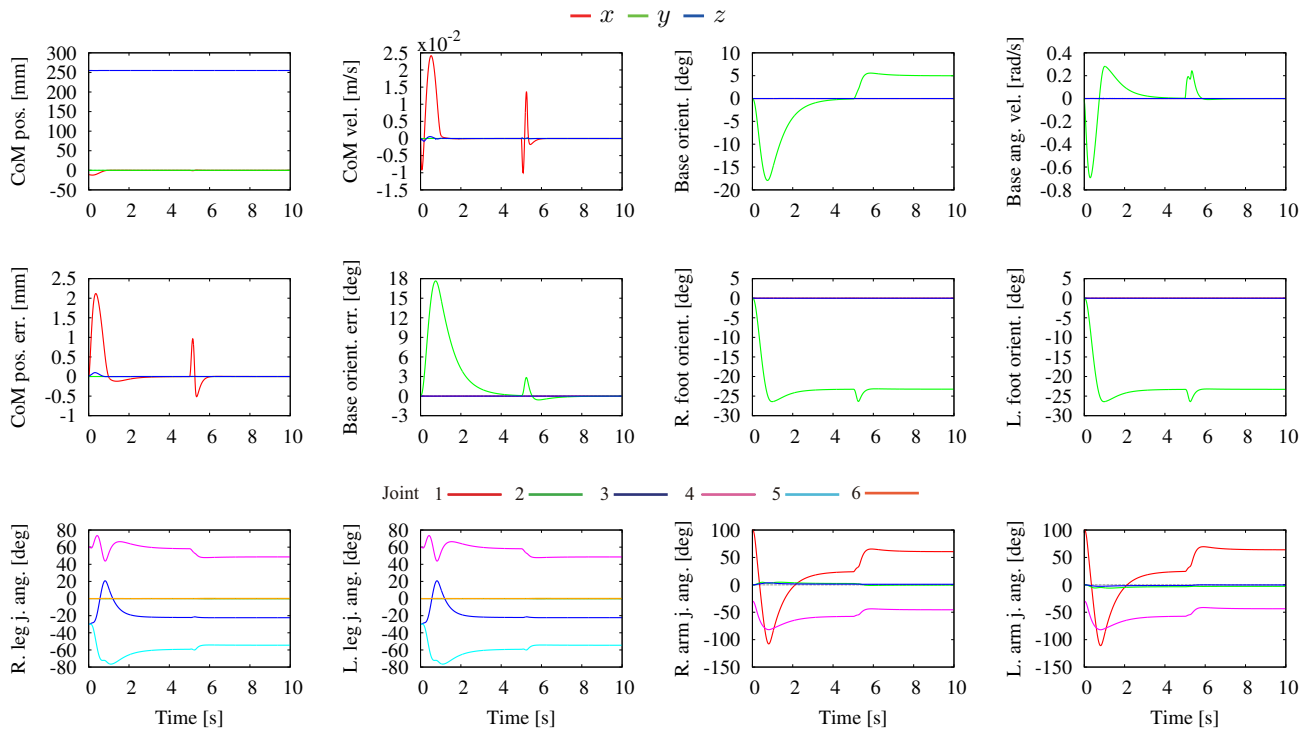


Fig. 5. RNS-based stabilization of a HOAP-2 robot model on a balance board. Initially, the CoM is slightly displaced from the vertical equilibrium line passing through the balance board center, yielding an unstable posture. Stabilization of the base-link requires about 5 s. After that, the robot self-destabilizes by a fast forward bent. The stabilization property of the controller can be reconfirmed for such type of destabilization. The joints of each limb are numbered in increasing order starting from the root link (the pelvis).

- [13] Toru Takenaka, Takashi Matsumoto, and Takahide Yoshiike. Real time motion generation and control for biped robot -3rd report: Dynamics error compensation-. In *IEEE/RSJ International Conference on Intelligent Robots and Systems*, pages 1594–1600, St. Louis, USA, oct 2009.
- [14] Johannes Engelsberger and Christian Ott. Integration of vertical COM motion and angular momentum in an extended Capture Point tracking controller for bipedal walking. In *IEEE-RAS International Conference on Humanoid Robots*, pages 183–189, 2012.
- [15] Sung-Hee Hee Lee and Ambarish Goswami. A momentum-based balance controller for humanoid robots on non-level and non-stationary ground. *Autonomous Robots*, 33(4):399–414, apr 2012.
- [16] Barkan Ugurlu and Atsuo Kawamura. Bipedal Trajectory Generation Based on Combining Inertial Forces and Intrinsic Angular Momentum Rate Changes: Eulerian ZMP Resolution. *IEEE Transactions on Robotics*, 28(6):1406–1415, 2012.
- [17] Johannes Engelsberger, Christian Ott, and Alin Albu-Schaffer. Three-dimensional bipedal walking control based on divergent component of motion. *IEEE Transactions on Robotics*, 31(2):355–368, apr 2015.
- [18] Georg Wiedebach, Sylvain Bertrand, Tingfan Wu, Luca Fiorio, Stephen McCrory, Robert Griffin, Francesco Nori, and Jerry Pratt. Walking on partial footholds including line contacts with the humanoid robot Atlas. In *IEEE-RAS International Conference on Humanoid Robots*, pages 1312–1319, nov 2016.
- [19] Dragomir N. Nenchev. Reaction Null Space of a multibody system with applications in robotics. *Mechanical Sciences*, 4:97–112, 2013.
- [20] M. W. Walker and D. E. Orin. Efficient dynamic computer simulation of robotic mechanisms. *Journal of Dynamic Systems, Measurement, and Control*, 104(3):205, 1982.
- [21] Richard M. Murray. Nonlinear control of mechanical systems: A Lagrangian perspective. *Annual Reviews in Control*, 21:31–42, 1997.
- [22] James P. Ostrowski. Computing reduced equations for robotic systems with constraints and symmetries. *IEEE Transactions on Robotics and Automation*, 15(1):111–123, 1999.
- [23] K. Mitobe, G. Capi, and Y. Nasu. Control of walking robots based on manipulation of the zero moment point. *Robotica*, 18(6):651–657, nov 2000.
- [24] T. Sugihara, Yoshihiko Nakamura, and H. Inoue. Real-time humanoid motion generation through ZMP manipulation based on inverted pendulum control. In *IEEE Int. Conf. on Robotics and Automation*, pages 1404–1409, Washington, DC, 2002.
- [25] Ryotaro Hinata and Dragomir N. Nenchev. Balance stabilization with angular momentum damping derived from the Reaction Null-Space. In *IEEE-RAS International Conference on Humanoid Robotics*, Beijing, PR China, 2018.
- [26] Anthony M. Bloch, Jerrold E. Marsden, and Dmitry V. Zenkov. Quasivelocities and symmetries in non-holonomic systems. *Dynamical Systems*, 24(2):187–222, 2009.
- [27] Sang-Ho Hyon, J.G. Hale, and Gordon Cheng. Full-body compliant human-humanoid interaction: balancing in the presence of unknown external forces. *IEEE Transactions on Robotics*, 23(5):884–898, oct 2007.
- [28] Bernd Henze, Máximo A. Roa, and Christian Ott. Passivity-based whole-body balancing for torque-controlled humanoid robots in multi-contact scenarios. *The International Journal of Robotics Research*, 35(12):1522–1543, oct 2016.
- [29] David E. Orin and Ambarish Goswami. Centroidal momentum matrix of a humanoid robot: Structure and properties. In *IEEE/RSJ International Conference on Intelligent Robots and Systems, IROS*, pages 653–659, Nice, France, 2008.
- [30] David E. Orin, Ambarish Goswami, and Sung Hee Lee. Centroidal dynamics of a humanoid robot. *Autonomous Robots*, 35(2-3):161–176, 2013.
- [31] Dragomir N. Nenchev. Differential Kinematics. In Ambarish Goswami and Prahlad Vadakkepat, editors, *Humanoid Robotics: A Reference*, pages 1–47. Springer Netherlands, Dordrecht, 2018.
- [32] A. Liegeois. Automatic supervisory control of the configuration and behavior of multibody mechanisms. *IEEE Transactions on Systems, Man, and Cybernetics*, 7(12):868–871, 1977.
- [33] Shin’Ichiro Nakaoka. Choreonoid: Extensible virtual robot environment built on an integrated GUI framework. In *IEEE/SICE International Symposium on System Integration (SII)*, pages 79–85, dec 2012.
- [34] Fujitsu. *Miniature humanoid robot HOAP-2 manual (in Japanese)*. Fujitsu Automation Co., Ltd, 1st edition, 2004.